A&A 452, 237–244 (2006)
DOI: 10.1051/0004-6361:20054522

Astronomy & Astrophysics

Circumstellar material in the Vega inner system revealed by CHARA/FLUOR

O. Absil[1,⋆], E. di Folco[2,3], A. Mérand[2], J.-C. Augereau[4], V. Coudé du Foresto[2], J. P. Aufdenberg[5], P. Kervella[2], S. T. Ridgway[5,6], D. H. Berger[6], T. A. ten Brummelaar[6], J. Sturmann[6], L. Sturmann[6], N. H. Turner[6], and H. A. McAlister[6]

[1] Institut d'Astrophysique et de Géophysique, Université de Liège, 17 Allée du Six Août, 4000 Liège, Belgium
e-mail: absil@astro.ulg.ac.be
[2] LESIA, UMR8109, Observatoire de Paris-Meudon, 5 place Jules Janssen, 92195 Meudon, France
[3] Observatoire de Genève, 51 chemin des Maillettes, 1290 Sauverny, Switzerland
[4] Laboratoire d'Astrophysique de l'Observatoire de Grenoble, UMR CNRS/UJF 5571, BP 53, 38041 Grenoble Cedex 9, France
[5] National Optical Astronomical Observatory, 950 North Cherry Avenue, Tucson, AZ 85719, USA
[6] Center for High Angular Resolution Astronomy, Georgia State University, PO Box 3969, Atlanta, Georgia 30302-3965, USA

Received 15 November 2005 / Accepted 6 February 2006

ABSTRACT

Context. Only a handful of debris disks have been imaged up to now. Due to the need for high dynamic range and high angular resolution, very little is known about the inner planetary region, where small amounts of warm dust are expected to be found.
Aims. We investigate the close neighbourhood of Vega with the help of infrared stellar interferometry and estimate the integrated K-band flux originating from the central 8 AU of the debris disk.
Methods. We performed precise visibility measurements at both short (∼30 m) and long (∼150 m) baselines with the FLUOR beam-combiner installed at the CHARA Array (Mt Wilson, California) in order to separately resolve the emissions from the extended debris disk (short baselines) and from the stellar photosphere (long baselines).
Results. After revising Vega's K-band angular diameter ($\theta_{\rm UD}$ = 3.202 ± 0.005 mas), we show that a significant deficit in squared visibility (ΔV^2 = 1.88 ± 0.34%) is detected at short baselines with respect to the best-fit uniform disk stellar model. This deficit can be either attributed to the presence of a low-mass stellar companion around Vega, or as the signature of the thermal and scattered emissions from the debris disk. We show that the presence of a close companion is highly unlikely, as well as other possible perturbations (stellar morphology, calibration), and deduce that we have most probably detected the presence of dust in the close neighbourhood of Vega. The resulting flux ratio between the stellar photosphere and the debris disk amounts to 1.29 ± 0.19% within the FLUOR field-of-view (∼7.8 AU). Finally, we complement our K-band study with archival photometric and interferometric data in order to evaluate the main physical properties of the inner dust disk. The inferred properties suggest that the Vega system could be currently undergoing major dynamical perturbations.

Key words. stars: individual: Vega – circumstellar matter – techniques: interferometric

1. Introduction

Vega (HD 172167, A0V, 7.76 pc) is probably one of the most important stars in astrophysics, as it has been used as a photometric standard for more than a century (Hearnshaw 1996). However, with the advent of infrared space-based telescopes, it was discovered to have a large infrared excess beyond 12 μm with respect to its expected photospheric flux (Aumann et al. 1984). This was identified as the thermal emission from a circumstellar disk of cool dust located at about 85 AU from Vega. Since this first discovery of a circumstellar dust around a main-sequence (MS) star, photometric surveys with IRAS (Fajardo-Acosta et al. 1999) and ISO (Laureijs et al. 2002) have shown that about 10% of MS stars have significant infrared excess in the 20−25 μm region.

Since the mid-1980s, great attention has been paid to Vega and other Vega-like stars. They have been imaged from the millimetric domain down to the visible, revealing circumstellar dust arranged in various shapes. For instance, Vega is known to be surrounded by a smooth annular structure similar to the solar Kuiper Belt, containing about 3×10^{-3} $M_\oplus$ of dust grains (Holland et al. 1998; Su et al. 2005), which also shows some clumpy components (Koerner et al. 2001; Wilner et al. 2002). However, due to the limitation in angular resolution of current telescopes, very little is known about the innermost part of these debris disks, which could potentially harbour warm dust ($\gtrsim$300 K) heated by the star as suggested by Fajardo-Acosta et al. (1998). Such warm dust would have a signature in the near- and mid-infrared that only photometric studies have attempted to detect until recently. Indeed, Vega's near-infrared (K, L, M) flux was shown to be significantly above the modelled photospheric level (Mountain et al. 1985), but this discrepancy was most likely due to an inadequate photospheric model since Vega's flux is consistent with other A-type stars to within standard photometric precision of 2−5% (Leggett et al. 1986). In the N band, the best constraint on the thermal emission from warm dust has been obtained by nulling interferometry, with no resolved emission above 2.1% of the level of stellar photospheric emission at

⋆ O.A. acknowledges the financial support of the Belgian National Fund for Scientific Research (FNRS).

Table 1. Individual measurements. Columns are: (1, 2) date and time of observation; (3, 4) projected baseline length and position angle (measured East of North); (5) squared visibility after calibration and error; (6, 9) HD number of calibrators used prior and after the given data point respectively, 0 means that there was no calibrator; (7, 8, 10, 11) quantities used for computing the correlation matrix as in Eq. (26) of Perrin (2003): σ_{V^2} are errors on the estimated visibility of the calibrators.

Date	UT	Projected baseline (m)	Position angle (°)	Calibrated V^2 (×100)	HD_a	α	$\sigma_{V_a^2}$	HD_b	β	$\sigma_{V_b^2}$
2005/05/21	06:17	101.60	−76.85	20.4 ± 1.14	0	0.000	0.000	165683	0.330	0.870
	07:31	127.86	−90.04	6.1 ± 0.25	176527	0.050	0.870	176527	0.060	1.025
	08:20	141.07	−97.43	2.6 ± 0.08	176527	0.026	1.025	173780	0.039	0.896
	08:59	148.55	−102.96	1.3 ± 0.04	173780	0.024	0.896	173780	0.017	0.895
2005/05/22	06:05	98.63	−75.25	23.2 ± 0.22	159501	0.240	0.467	159501	0.064	0.624
	06:24	105.77	−79.02	18.2 ± 0.20	159501	0.142	0.467	159501	0.101	0.624
	06:29	107.70	−80.00	16.8 ± 0.18	159501	0.120	0.467	159501	0.107	0.624
	06:39	111.61	−81.97	14.4 ± 0.15	159501	0.082	0.467	159501	0.115	0.624
	06:49	115.39	−83.83	12.2 ± 0.14	159501	0.052	0.467	159501	0.117	0.624
	06:59	118.79	−85.51	10.4 ± 0.12	159501	0.030	0.467	159501	0.115	0.624
	08:18	141.45	−97.68	2.6 ± 0.07	173780	0.014	0.624	173780	0.051	0.897
	08:23	142.62	−98.45	2.4 ± 0.06	173780	0.011	0.624	173780	0.051	0.897
	08:34	144.75	−99.93	2.0 ± 0.06	173780	0.005	0.624	173780	0.049	0.897
2005/06/13	05:22	33.59	20.55	84.2 ± 1.42	168775	0.543	0.152	168775	0.362	0.153
	06:15	33.85	13.58	83.4 ± 0.92	168775	0.269	0.153	168775	0.628	0.153
	06:46	33.92	9.33	84.5 ± 0.73	168775	0.419	0.153	163770	0.523	0.272
	07:14	33.96	5.49	80.8 ± 0.99	163770	0.510	0.272	163770	0.419	0.272
	07:43	33.97	1.37	82.8 ± 1.35	163770	0.514	0.272	163770	0.438	0.272
	08:13	33.97	−2.95	84.5 ± 1.19	163770	0.833	0.272	168775	0.129	0.152
	09:37	33.82	−14.54	83.6 ± 0.67	163770	0.123	0.272	168775	0.784	0.152
	10:04	33.70	−18.05	83.9 ± 0.66	168775	0.574	0.152	176670	0.330	0.167
2005/06/14	07:58	33.98	−1.26	85.0 ± 0.90	176670	0.521	0.166	176670	0.400	0.166
2005/06/15	06:03	33.83	14.15	84.4 ± 1.16	176670	0.458	0.167	176670	0.457	0.167
	06:39	33.92	9.18	86.5 ± 1.35	176670	0.363	0.167	176670	0.575	0.166
	07:07	33.96	5.37	84.2 ± 1.41	176670	0.544	0.166	163770	0.392	0.272

separations larger than 0.8 AU (Liu et al. 2004). At longer wavelengths, the recent measurements obtained with Spitzer in the far-infrared (Su et al. 2005) have not allowed for an investigation of the inner part of Vega's disk because of the limited resolution (47 AU at the distance of Vega) and because hot dust is not expected to contribute significantly to the far-infrared flux.

In this paper, we use infrared stellar interferometry to investigate the inner part of Vega's debris disk. Such an attempt had already been made by Ciardi et al. (2001), who observed Vega with the PTI interferometer on a 110 m long baseline in dispersed mode. The poor spatial frequency coverage of their observations did not allow clear conclusions, although a simple model of a star and a uniform dust disk with a 3−6% flux ratio was proposed to explain the observations. A more thorough study of Vega-type stars was performed with the VLTI by di Folco et al. (2004), using short and long baselines to separately resolve the two components of the system (stellar photosphere at long baselines and circumstellar emission at short baselines). Unfortunately, the visibility precision and the available baselines at the VLTI only allowed upper limits to be inferred on the flux of the inner disks. In order to better constrain the near-infrared brightness of Vega's disk, we have used the same method at the CHARA Array (ten Brummelaar et al. 2005) with an optimised set of baselines.

2. Observations and data reduction

Interferometric observations were obtained in the infrared K band (1.94−2.34 μm) with FLUOR, the Fiber Linked Unit for Optical Recombination (Coudé du Foresto et al. 2003), using the S1–S2 and E2–W2 baselines of the CHARA Array, 34 and 156 m respectively. Observations took place during Spring 2005, on May 21st and May 22nd for E2–W2, and between June 13th and June 15th for S1–S2 (see Table 1). The FLUOR field-of-view, limited by the use of single-mode fibers, has a Gaussian shape resulting from the overlap integral of the turbulent stellar image with the fundamental mode of the fiber (Guyon 2002). Under typical seeing conditions, it has a radius of 1″ (distance at which the coupling efficiency falls to 3% of its on-axis value).

Table 2. Calibrators with spectral type, K magnitude, limb-darkened disk (LD) angular diameter in K band (in milliarcsec) and baseline (Bordé et al. 2002; Mérand et al. 2005).

	S. type	K mag	LD diam. (mas)	Baseline
HD 159501	K1 III	3.14	1.200 ± 0.014	E2–W2
HD 163770	K1 IIa	1.03	3.150 ± 0.034	S1–S2
HD 165683	K0 III	2.9	1.152 ± 0.014	E2–W2
HD 168775	K2 IIIab	1.74	2.280 ± 0.025	S1–S2
HD 173780	K2 III	2.0	1.950 ± 0.021	E2–W2
HD 176527	K2 III	2.04	1.765 ± 0.024	E2–W2
HD 176670	K2.5 III	1.6	2.410 ± 0.026	S1–S2

The FLUOR Data Reduction Software (Coudé du Foresto et al. 1997; Kervella et al. 2004) was used to extract the squared modulus of the coherence factor between the two independent apertures. The interferometric transfer function of the instrument was estimated by observing calibrators before and after each Vega data point. All calibrator stars (Table 2) were chosen from two catalogues developed for this specific purpose (Bordé et al. 2002; Mérand et al. 2005). Calibrators chosen in this study are all K giants, whereas Vega is an A0 dwarf. The spectral type difference is properly taken into account in the Data Reduction Software, even though it has no significant influence on the final result. The efficiency of CHARA/FLUOR was consistent

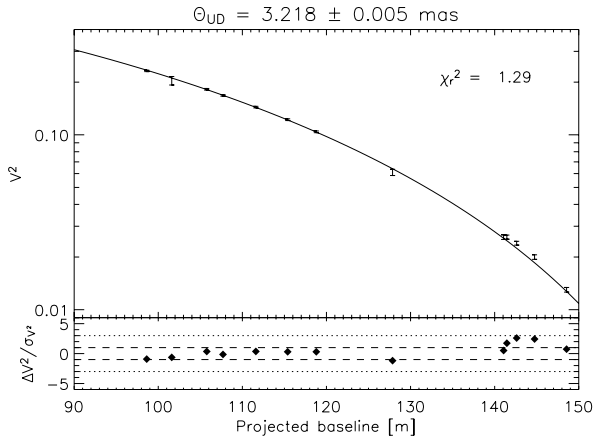

Fig. 1. Fit of a uniform stellar disk model to the E2–W2 data. The quality of the fit is satisfactory (reduced χ^2 of 1.29), with small residuals that do not display any obvious trend except for a small underestimation of the actual data for baselines between 140 and 150 m.

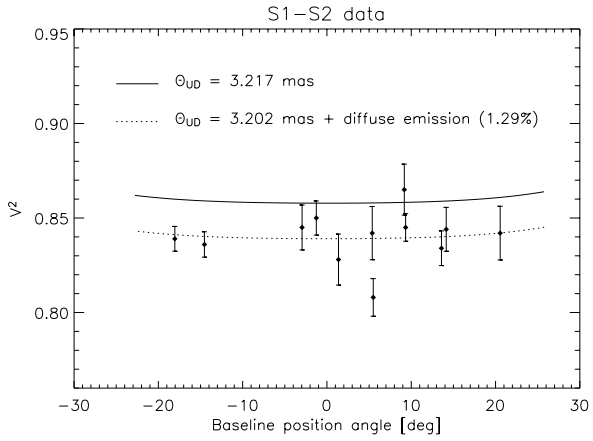

Fig. 2. The data obtained with the S1–S2 baseline (~34 m) are displayed as a function of the projected baseline's position angle together with the best UD fit computed over the whole data set (3.217 mas). The data points are significantly below the best UD fit, with a mean visibility deficit $\Delta V^2 \simeq 2\%$. The addition of a uniform diffuse source of emission in the FLUOR field-of-view reconciles the best fit with the data (dotted line). Note that there is no obvious dependence of the data points with respect to position angle, which would be indicative of an asymmetric extended emission.

between all calibrators and stable night after night to around 85%. Data that share a calibrator are affected by a common systematic error due to the uncertainty of the a priori angular diameter of this calibrator. In order to interpret our data properly, we used a specific formalism (Perrin 2003) tailored to propagate these correlations into the model fitting process. All diameters are derived from the visibility data points using a full model of the FLUOR instrument including the spectral bandwidth effects (Kervella et al. 2003).

3. Data analysis

3.1. Stellar diameter

The measurements obtained with the long E2–W2 baseline are particularly appropriate for a precise diameter determination, because they provide good spatial frequency coverage of the end of the first lobe of the visibility curve (see Fig. 1). Previous interferometric measurements obtained in the visible by Hanbury Brown et al. (1974) and Mozurkewich et al. (2003) were used to derive uniform disk (UD) diameters $\theta_{\rm UD} = 3.08 \pm 0.07$ ($\lambda = 440$ nm) and $\theta_{\rm UD} = 3.15 \pm 0.03$ ($\lambda = 800$ nm) respectively. In the K band, where the limb-darkening effect is not as strong, Ciardi et al. (2001) estimated the UD diameter to be $\theta_{\rm UD} = 3.24 \pm 0.01$ mas. We have fitted a uniform stellar disk model to our E2–W2 data, assuming that Vega's photospheric intensity $I(\phi, \lambda)$ equals the Planck function with an effective temperature of 9550 K for all angles ϕ. The best-fit diameter is $\theta_{\rm UD} = 3.218 \pm 0.005$ mas for an effective wavelength of 2.118 μm, which significantly revises the previously obtained estimates[1]. The quality of the fit is quite good ($\chi^2_r = 1.29$). Unlike in the PTI data of Ciardi et al. (2001), we do not see any obvious trend in the residuals of the fit, except for three points at projected baselines between 140 and 150 m which are slightly above the fit (by ~1.5σ). In fact, Fig. 3 not only shows a significant discrepancy between the CHARA/FLUOR and the PTI data, but also between the 1999 and 2000 PTI data. Our observations do not support the scenario of Ciardi et al. (2001), who proposed a uniform dust ring with a 3–6% integrated flux relative to the Vega photosphere in K band to account for the trend that they observed in the residuals of the fit obtained with a simple limb-darkened disk (LD) stellar model.

Note that fitting an LD stellar model to our data would only marginally improve the fit (see Table 3), as the shape of the first-lobe visibility curve is not very sensitive to limb darkening. Moreover, the actual limb-darkening parameter may be significantly larger than standard tabulated values because Vega is suspected to be a fast rotating star viewed nearly pole-on and the equatorial darkening may bias the limb profile (Gulliver et al. 1994; Peterson et al. 2004). Complementary observations to our data set, obtained by Aufdenberg et al. (2006) at ~250 m baselines, confirm this fact and lead to an accurate estimation of the K-band limb profile, which mostly affects visibilities beyond the first null and will not be discussed here.

3.2. Visibility deficit at short baselines

With this precise diameter estimation, we can now have a look at the short-baseline data. In fact, these points do not significantly contribute to the UD fit because of the low spatial frequencies they sample. Including all the data points in the fitting procedure gives a best-fit diameter $\theta_{\rm UD} = 3.217 \pm 0.013$ mas, but with a poor $\chi^2_r = 3.36$. We show the reason for this poor reduced χ^2 in Fig. 2, where the S1–S2 data points are plotted as a function of position angle together with the best UD fit (solid line). The observations are consistently below the fit, with a $\Delta V^2 = 1.88 \pm 0.34\%$.

Systematic errors in the estimation of the calibrator diameters or limb-darkened profiles are possible sources of bias in interferometric observations. In order to explain the measured visibility deficit in the S1–S2 data, the diameters of the three short-baseline calibrators (Table 2) should have been underestimated by 0.26, 0.35 and 0.33 mas respectively, which represent about 10 times the estimated error on their diameters. We have made sure that such improbable errors were not present in our calibration procedure by cross-calibrating the three calibrators. No significant departure from the expected LD diameters was measured, and the calibrated visibilities of Vega do not

[1] The K-band diameter proposed by Ciardi et al. (2001) was computed with the assumption of a flat spectrum for the Vega intensity. This explains a large part of the discrepancy with our new value.

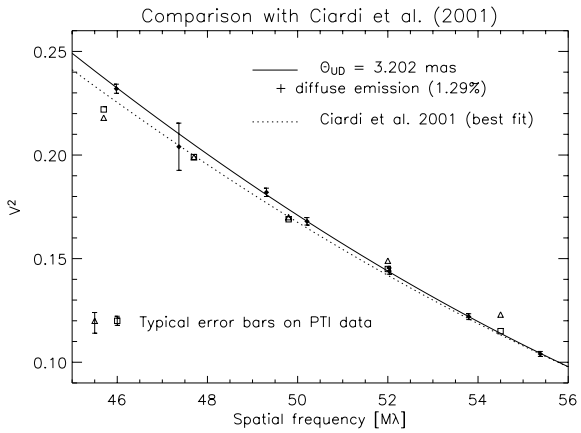

Fig. 3. Comparison of our E2-W2 data (black dots) with the observations of Ciardi et al. (2001) obtained at PTI (triangles: data acquired in 1999, squares: data acquired in 2000). The data are displayed as a function of spatial frequency, taking an equivalent wavelength of 2.145 μm for the FLUOR instrument (computed for a flat stellar spectrum as in the study of Ciardi et al. 2001). The 1σ errors on the PTI data are shown at the bottom of the figure for the sake of clarity.

Table 3. Influence of the limb-darkening parameter α on the best-fit diameter and the associated reduced χ^2 using the whole data set, assuming a brightness distribution $I(\mu) = \mu^\alpha$ with $\mu = \cos\theta$ the cosine of the azimuth of a surface element of the star (Hestroffer 1997). The visibility deficit measured at short baselines (S1–S2) with respect to the best-fit model is given in the last column, showing a weak dependence on the limb-darkening model.

α	Best-fit θ_{LD} (mas)	χ^2_r (all data)	ΔV^2 (S1–S2)
0.0	3.217 ± 0.013	3.36	1.88%
0.1	3.264 ± 0.013	3.14	1.83%
0.2	3.310 ± 0.012	2.96	1.78%
0.3	3.356 ± 0.012	2.82	1.73%
0.4	3.402 ± 0.011	2.71	1.67%
0.5	3.447 ± 0.011	2.64	1.62%
0.6	3.491 ± 0.011	2.61	1.58%
0.7	3.536 ± 0.012	2.60	1.53%
0.8	3.579 ± 0.012	2.62	1.49%
0.9	3.623 ± 0.012	2.66	1.44%

depend on the chosen calibrator. Therefore, it appears extremely unlikely that the calibration process may have induced the observed visibility deficit.

A limb-darkened stellar model for Vega will not reconcile the best-fit stellar model with the S1–S2 data points (see Table 3), because low spatial frequencies are not sensitive to limb darkening. One may think of stellar asymmetry as a possible reason for the visibility deficit at short baselines, since the position angles of the short and long baselines are almost perpendicular (see Table 1). However, an oblateness ratio of 1.07 for Vega would be needed to explain the deficit, which would strongly contradict previous interferometric studies (van Belle et al. 2001; Peterson et al. 2004). Other stellar features such as spots would not explain this deficit either as they can only appear in the second and higher lobes of the visibility function. In fact, a natural explanation to the observed visibility deficit would be the presence of an extended source of emission in the interferometric field-of-view (e.g. disk or companion), which would be resolved with the S1–S2 baseline (i.e., incoherent emission).

In order to assess the amount of incoherent emission needed to explain the observed visibility deficit, we have added a diffuse emission, uniformly distributed in the CHARA/FLUOR field-of-view, to our UD stellar model. Fitting this new model to the complete data set gives the following final result: θ_{UD} = 3.202 ± 0.005 mas, K-band flux ratio = 1.29 ± 0.19%, with a significantly decreased χ^2_r = 1.10 (instead of 3.36). This result is almost independent of the extended source morphology, as the spatial frequency coverage of our interferometric data is too scarce to constrain its spatial distribution. The extended structure, detected with very good confidence (almost 7σ), would thus have a relative flux contribution of 1.29% with respect to the Vega photosphere in K band when integrated over the whole field-of-view (7.8 AU in radius). Such an excess does not contradict photometric measurements in the K band, which have typical accuracies of 2–3% (Mégessier 1995). The result of the fit is displayed in Fig. 2 (dotted line) and Fig. 3 (solid line), as well as in Fig. 4 for a realistic debris disk model (see Sect. 4.2), which gives the same best-fit parameters.

4. Discussion

In this section, we discuss the possible sources of incoherent flux around Vega that could account for the observed visibility deficit at short baselines.

4.1. Point source

Because of our sparse sampling of spatial frequencies, a point source located in the FLUOR field-of-view could also be the origin of the observed visibility deficit. Regardless of the bound or unbound character of the companion, there are essentially two regimes to be considered when computing the visibility of a binary system, depending on whether the fringe packet associated with the companion falls into the FLUOR observation window or not. The observation window is defined as the total optical path L_{OPD} scanned by the FLUOR dither mirror, which is used to temporally record the fringes. The secondary fringe packet lies outside the observation window if $|B\,\alpha\cos\theta| > L_{OPD}/2$, where B is the baseline length, α the angular separation of the binary system, θ the angle between the baseline and the orientation of the binary system, and L_{OPD} = 102 μm. In that case, e.g. for an angular separation larger than 350 mas at a baseline of 34 m, the flux from the secondary will contribute incoherently and will lead to the same signature as a diffuse emission in the FLUOR field-of-view. A binary star with a separation ranging between 350 and 1000 mas could therefore reproduce the observed visibilities. On the other hand, if the secondary fringe packet is inside the observation window, it will lead either to a visibility modulation of twice the flux ratio as a function of baseline azimuth if the fringe packets are superposed, or to an enhancement of the measured visibility if the fringe packets are separated. Even if such behaviour does not seem compatible with the observed visibilities, our sparse data cannot definitely rule out a solution with a close companion.

The presence of a point source located within the FLUOR field-of-view could thus possibly explain our observations. The minimum K-band flux ratio between the point source and Vega is 1.29 ± 0.19%, valid for a very close companion ($\lesssim$50 mas). Because of the Gaussian shape of the off-axis transmission, the companion would have a larger flux if located farther away from the star. For instance, the flux should be increased by 10% at 100 mas, by 50% at 200 mas and by 3000% at 500 mas from the star in order to reproduce the observed visibility deficit.

Based on a minimum K-band flux ratio of 1.29 ± 0.19% and a K magnitude of 0.02 for Vega (Mégessier 1995), we deduce an upper limit of $K = 4.74 \pm 0.17$ for a companion.

4.1.1. Field star

Although Vega is known to be surrounded by a number of faint objects ($V > 9$) with low proper motion since the beginning of the 20th century (Dommanget & Nys 2002), these objects are far enough from Vega (at least 1′) so that they do not interfere with our measurements. In the infrared, neither adaptive optics studies (Macintosh et al. 2003; Metchev et al. 2003) nor the 2MASS survey (Cutri et al. 2003) identified any $K < 5$ object within 1′ of Vega. In fact, the local density of such objects is about 5×10^{-4} per arcmin^2 according to the 2MASS survey, so that the probability to find a $K < 5$ source within 1″ of Vega is smaller than 4.3×10^{-7}.

4.1.2. Physical companion

At the distance of Vega, the putative companion would have a maximum absolute magnitude $M_K = 5.15 \pm 0.17$. Assuming this companion to be a star of the same age as Vega itself, comprised between 267 and 383 Myr (Song et al. 2001), we use the evolutionary models developed by Baraffe et al. (1998) to deduce the range of effective temperature and mass for the companion: $T_{\rm eff} = 3890 \pm 70$ K and $\mathcal{M} = 0.60 \pm 0.025\ \mathcal{M}_\odot$. This roughly corresponds to an M0V star (Delfosse et al. 2000).

With a $V - K$ of 3.65 (Bessel & Brett 1988), the M0V companion would have a V magnitude of 8.41 and would therefore have remained undetected in high resolution visible spectra of Vega (M. Gerbaldi, personal communication). Adaptive optics studies in the near-infrared would not have noticed the companion either, due to its very small angular distance from the bright Vega (<1″). At longer wavelengths, the expected infrared excess due to an M0V companion is not large enough to be detected by classical photometry as its does not exceed 2% between 10 and 100 μm. Indirect methods are in fact much more appropriate to detect this kind of companion.

Astrometric measurements of Vega with Hipparcos did not detect the presence of any companion, with an astrometric precision of 0.5 mas (Perryman 1997). With a mass ratio of 4.2 between Vega (2.5 $\mathcal{M}_\odot$) and its putative M0V companion (0.6 $\mathcal{M}_\odot$), a 3σ astrometric stability of 1.5 mas implies that the orbital semi-major axis of the putative companion cannot be larger than 6.3 mas[2] (=0.05 AU = 4 $R_\star$) with a 99% confidence assuming a circular orbit, which is anticipated for such a small separation. Such a close companion, which could also fit the interferometric data, would have an appreciable signature in radial velocity measurements, unless the binary system is seen almost exactly pole-on. Precise measurements recently obtained with the ELODIE spectrometer have shown a relative stability of Vega's radial velocity over several months, with amplitudes lower than 100 m/s and a precision of order of 30 m/s each (F. Galland, private communication). Assuming that the orbital plane of the M0V companion is perpendicular to Vega's rotation axis, inclined by 5.1° with respect to the line-of-sight (Gulliver et al. 1994), the companion should be farther than 80 AU from Vega to be compatible with the measured radial velocity stability. In fact, for an M0V companion at 0.05 AU from Vega not to display any radial velocity signature at the 100 m/s level, its orbital inclination needs to coincide with the plane of the sky to within ±0.13° (Perryman 2000). Even if such an inclination is possible, the probability for the system to be so close to pole-on is very low (it ranges between about 6×10^{-4} and 10^{-6} depending on the assumptions on the statistical distribution of low-mass companion orbital planes). In conclusion, even though the presence of an M0V companion close to Vega could explain the interferometric data, there is strong evidence that such a companion does not exist.

[2] The astrometric signature of a low-mass companion is given by the ratio between the orbital semi-major axis and the mass ratio (Perryman 2000).

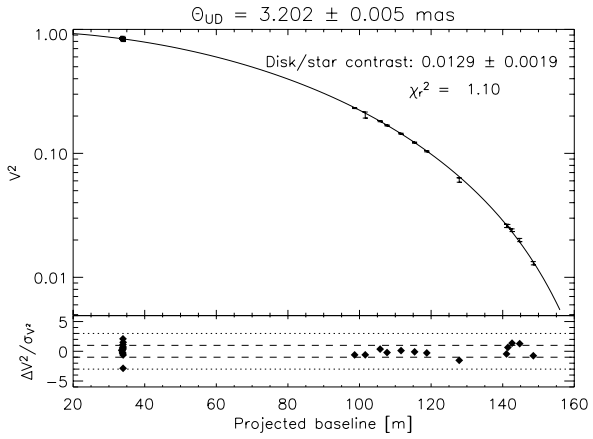

Fig. 4. Fit of a uniform stellar disk + circumstellar disk model to our full data set, using the model of Kelsall et al. (1998).

4.2. Circumstellar material

Circumstellar disks around MS stars are understood to be composed of second-generation dust grains originating from collisions between small bodies (asteroids) or from the evaporation of comets (Backman & Paresce 1993). They are assumed to be continuously replenished since dust grains have a limited lifetime (<10 Myr) due to radiation pressure, Poynting-Robertson (P-R) drag and collisional destruction (Dominik & Decin 2003). Several studies have shown Vega to harbour a cold circumstellar dust ring ~85 AU in radius (Holland et al. 1998; Heinrichsen et al. 1998; Koerner et al. 2001; Wilner et al. 2002). Su et al. (2005) interpreted the extended dust emission (up to 600 AU, i.e., 77″) detected by Spitzer as the signature of dust grains being expelled by radiation pressure from the Vega system as a result of a recent collision in the main planetesimal ring and subsequent collisional cascade. Even if the presence of dust in the inner part of the disk has not been detected yet due to instrumental limitations, an equivalent to the solar zodiacal cloud is expected to be found around Vega. The thermal and scattered emissions from warm grains surrounding Vega could thus be a natural explanation to the visibility deficit observed at short baselines, provided that a sufficient quantity of dust is present within 8 AU from the star.

In order to assess the adequacy of a circumstellar disk to reproduce the observations, we have fitted our full data set with the only known model for an inner debris disk, i.e., the zodiacal disk model of Kelsall et al. (1998)[3], assuming that the inner dust distribution around Vega follows the same density and temperature power-laws as for the solar zodiacal cloud. The result is displayed in Fig. 4 wherein all data points are nicely spread

[3] This model was implemented in an IDL package called ZODIPIC by M. Kuchner (`http://www.astro.princeton.edu/~mkuchner/`).

Table 4. Available constraints on the near- and mid-infrared excess around Vega. References: (1) Campins et al. (1985); (2) Blackwell et al. (1983); (3) Rieke et al. (1985); (4) Liu et al. (2004); (5) Cohen et al. (1992), with the absolute photometric error estimated by Aumann et al. (1984). The photometric data in references (1), (2) and (3) have been compared to the most recent Kurucz photospheric model of Vega (Bohlin & Gilliland 2004), which has a typical uncertainty of 2% in the infrared (this uncertainty has been added to the estimated errors on the measurements). Note that the interferometric data from FLUOR and BLINC only sample a specific part of the inner disk, while the photometric studies include Vega's entire environment.

Wavelength	Excess	Instruments	References
1.26 μm	2.4 ± 2.9%	Catalina, UKIRT	(1), (2)
1.60 μm	−2.4 ± 3.6%	Catalina	(1)
2.12 μm	1.29 ± 0.19%	CHARA/FLUOR	This study
2.20 μm	4.1 ± 3.0%	Catalina, UKIRT	(1), (2)
3.54 μm	3.1 ± 3.0%	Catalina, UKIRT	(1), (2)
4.80 μm	7.1 ± 5.1%	Catalina, UKIRT	(1), (2)
10 μm	6 ± 4.5%	Various	(3)
10.6 μm	0.2 ± 0.7%	MMT/BLINC	(4)
12 μm	1.2 ± 5%	IRAS	(5)

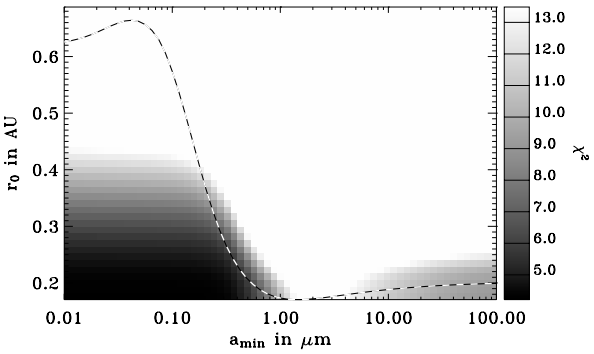

Fig. 5. Map of the χ^2 as a function of minimum grain size $a_{\rm min}$ and inner radius r_0, obtained by fitting the circumstellar disk model of Augereau et al. (1999) to the SED data of Table 4. We have assumed a surface density power-law $\Sigma(r) \propto r^{-4}$ and a grain size distribution $dn(a) \propto a^{-3.7}da$, with a maximum size of 1500 μm. In this simulation, the disk is composed of 50% amorphous carbons and 50% glassy olivines (see text). The dashed line represents the distance at which sublimation happens for dust grains of a given size (isotherm T = 1700 K). The axis labels should therefore read "a in μm" and "sublimation radius in AU" for this curve.

around the best-fit model (as expected, because our interferometric data are not sensitive to the particular morphology of the incoherent emission). The long-baseline data are also better fitted than with a simple UD model, because the presence of the dust disk has some influence on the slope of the visibility curve at long baselines (di Folco et al. 2004). The resulting flux ratio between the whole circumstellar disk and the stellar photosphere (1.29 ± 0.19%) is the same as with a simple model of uniform diffuse emission (Sect. 3.2), with the same reduced χ^2 of 1.10. Using the model of Kelsall et al. (1998), a flux ratio of 1.29% in K band would suggest that the dust density level in the inner Vega system is about 3000 times larger than in the solar zodiacal cloud. However, we will see later on that this model is not appropriate to represent Vega's inner disk (it would largely overestimate its mid-infrared flux), so that the comparison is not actually pertinent.

4.2.1. Physical properties of the dust grains

Let us now try to evaluate the main physical properties of the dust grains in the inner debris disk. Table 4 gives the photometric constraints on the near- and mid-infrared excess flux around Vega currently available in the literature. Photometric constraints at wavelengths longer than 12 μm are not appropriate for our purpose as they are mostly sensitive to the cold outer disk (the inner disk is not supposed to produce a significant photometric contribution in the far-infrared). The large error bars on the photometric measurements take into account both the actual error on photometric measurements and the estimated accuracy of photospheric models for Vega, to which the measurements are compared. Our study is compatible with previous near-infrared measurements but provides a much stronger constraint on the inner disk, because interferometry spatially resolves the disk from the stellar photosphere and focuses on the inner part of the disk thanks to the small field-of-view. Nulling interferometry at the MMT with the BLINC instrument also provides a valuable constraint on the mid-infrared excess (Liu et al. 2004). The sinusoidal transmission map of this nulling interferometer restricts however the observation to the part of the disk located farther than about 125 mas (∼1 AU) from the star. This explains why the result of this study is significantly below the estimated mid-infrared photometric excesses, as it is not sensitive to hot grains in the innermost part of the disk.

We have tried to reproduce the Spectral Energy Distribution (SED) of the infrared excess as listed in Table 4 with the debris disk model developed by Augereau et al. (1999). For that purpose, we took for Vega a NextGen model atmosphere spectrum (Hauschildt et al. 1999) with $T_{\rm eff}$ = 9600 K and $\log(g)$ = 4.0, scaled to match the observed visible magnitude (V = 0.03) at a distance of 7.76 pc, which gives a luminosity of 58.7 $L_\odot$. Various grain compositions and size distributions were used in the disk model, as well as various radial density profiles, assuming no azimuthal dependence. In each model, the sublimation temperature of the grains is set to $T_{\rm sub}$ = 1700 K. At a given distance and for a given size distribution, only grains large enough to survive the sublimation process can actually coexist (see dashed curve in Fig. 5). The normalised differential size distribution between $a_{\rm min}$ and $a_{\rm max}$ (fixed) is thus truncated at $a_{\rm sub}$, which depends on the radial distance to the star. For each model, a χ^2 map is computed for all possible values of $a_{\rm min}$ (minimum grain size) and r_0 (inner radius where the disk is artificially truncated), adjusting the surface density at r_0 by a least-squares method (see Fig. 5). The most constraining observations in this process are the two interferometric measurements at 2.12 and 10.6 μm, so that the fitting procedure mainly boils down to adjusting the near-infrared flux without producing a too strong 10.6 μm emission feature. Comparison of χ^2 values allowed us to infer most probable physical properties for the inner debris disk.

– **Size distribution:** the inner disk seems to be mainly composed of hot (∼1500 K) and small (<1 μm) dust grains, which emit mostly in the near-infrared. Although larger grains (≥10 μm) cannot be ruled out as the main source of the excess, such grains generally produce too large a mid-infrared flux as they emit more efficiently in this wavelength range. This suggests a steep size distribution with a small minimum grain size ($a_{\rm min} \leq$ 0.3 μm, assuming compact grains). For instance, we find that a size distribution similar to that inferred by Hanner (1984) for cometary grains provides a good fit to the SED, as well as the interstellar size

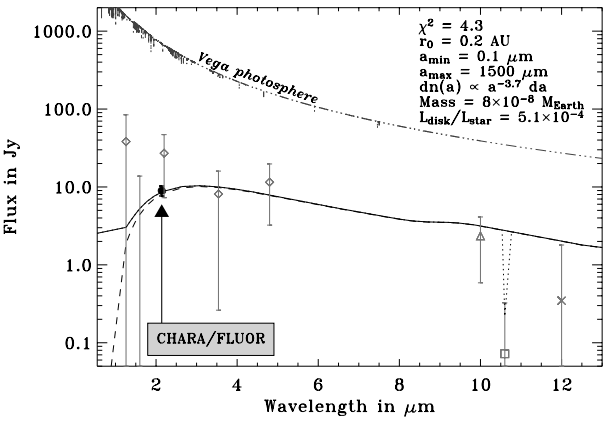

Fig. 6. A possible fit of our debris disk model (Augereau et al. 1999) to the photometric and interferometric constraints of Table 4: the diamonds correspond to references (1) and (2), the filled circle to this study, the triangle to (3), the square to (4) and the cross to (5). The model used here has a size distribution $\mathrm{d}n(a) \propto a^{-3.7}\mathrm{d}a$ with limiting grain sizes $a_{\min} = 0.1$ μm and $a_{\max} = 1500$ μm, a surface density power-law $\Sigma(r) \propto r^{-4}$ with an inner radius $r_0 = 0.2$ AU, and assumes a disk composed of 50% amorphous carbon and 50% glassy olivine. The solid and dotted lines represent the total emission from the disk on a 8 AU field-of-view, respectively without and with the spatial filtering of interferometric studies, while the dashed line takes only the thermal emission into account. The photospheric SED, simulated by a NextGen model atmosphere (see text), is represented as a dashed-dotted line for comparison.

distribution of Mathis et al. (1977). Both have power-law exponents of −3.5 or steeper. On the contrary, the size distribution of Grün et al. (1985) for interplanetary dust particles does not provide a good reproduction of the disk's SED, so that the grain size distribution is most probably different from that of the solar zodiacal cloud described by Reach et al. (2003).

– **Composition:** large amounts of highly refractive grains, such as graphites (Laor & Draine 1993) or amorphous carbons (Zubko et al. 1996), are most probably present in the inner disk. This is required in order to explain the lack of significant silicate emission features around 10 μm (Gaidos & Koresko 2004), which are especially prominent for small grains. Silicate grains can still be present in the disk, but with a maximum volume ratio of ∼70%, using the astronomical silicates of Weingartner & Draine (2001) or the glassy olivines ($Mg_{2y}Fe_{2-2y}SiO_4$) of Dorschner et al. (1995) with $y = 0.5$. This is another difference from the solar zodiacal cloud, which is thought to contain about 90% of silicate grains (Reach et al. 2003). Such a mixing ratio would only be possible around Vega if the grains were sufficiently big ($a_{\min} \geq 10$ μm), so that the silicate emission feature around 10 μm would not be too prominent.
– **Density profile:** the inner radius r_0 of the dusty disk is estimated to be between 0.17 and 0.3 AU. Assuming a sublimation temperature of 1700 K, dust grains larger than 0.5 μm would survive at such distances (see dashed curve in Fig. 5) while smaller grains, which are hotter, sublimate farther from the star (e.g. at ∼0.6 AU for a 0.1 μm grain). A steep power-law for the radial surface density distribution has also been inferred from our investigations. A power-law exponent of −4 or steeper provides a good fit to the SED, as it reduces the amount of dust in the regions farther than 1 AU and thereby explains the non-detection with MMT/BLINC reported by Liu et al. (2004). In contrast, the zodiacal disk model of Kelsall et al. (1998) has a flat surface density power-law with an exponent around −0.34.

Using these most probable parameters for the inner disk and a mixed composition of 50% amorphous carbons (Zubko et al. 1996) and 50% glassy olivines ($MgFeSiO_4$, Dorschner et al. 1995), we have obtained a relatively good fit to the SED as illustrated in Fig. 6, where we see that the thermal emission from the hot grains supersedes the contribution from scattered light at wavelengths longer than 1.3 μm. Based on our model and assuming a size distribution $\mathrm{d}n(a) \propto a^{-3.7}\mathrm{d}a$ with $a_{\min} = 0.1$ μm and $a_{\max} = 1500$ μm, we can deduce estimations for the dust mass in the inner 10 AU of the disk ($\mathcal{M}_{\mathrm{dust}} \sim 8 \times 10^{-8}$ $\mathcal{M}_{\oplus}$, equivalent to the mass of an asteroid about 70 km in diameter) and for the bolometric luminosity ratio between the inner disk and the star ($L_{\mathrm{disk}}/L_{\star} \sim 5 \times 10^{-4}$). Because of the high temperature of the grains, the luminosity of the inner disk is more than one order of magnitude larger than the luminosity of the outer disk estimated by Heinrichsen et al. (1998), even though it is almost 10^5 times less massive than the outer disk. These results need to be confirmed by future studies, as the SED of the inner disk is still relatively poorly constrained. They have been included in this paper to demonstrate that the presence of warm circumstellar dust can reproduce the various observations, and to provide a plausible dust-production scenario as discussed below.

4.2.2. A possible scenario for the presence of hot dust

In fact, three main scenarios may explain the presence of small dust grains so close to Vega. As in the case of the solar zodiacal cloud, they could be produced locally, e.g. by collisions between larger bodies arranged in a structure similar to the solar asteroidal belt. Another local source of small grains is the evaporation of comets originating from the reservoir of small bodies at ∼85 AU from Vega or from an inner population of icy bodies as in the case of β Pic (Beust & Morbidelli 2000). Finally, dust grains produced by collisions in the outer disk could drift towards the inner region because of P-R drag. However, this latter scenario cannot be connected to the recent collision(s) in the outer disk suggested by Su et al. (2005), because of the long timescale of P-R drag (2×10^7 yr, Dent et al. 2000). Moreover, due to the much shorter collisional timescale (5×10^5 yr in the outer disk), this process is not very efficient and is therefore unlikely to produce the observed amount of dust in Vega's inner system. Our observations cannot discriminate between the two remaining scenarios, even though a cometary origin is favoured by the steep size distribution of dust grains (Hanner 1984) and by the small inner disk radius.

Due to radiation pressure, small grains will not survive in the Vega inner disk more than a few years before being ejected toward cooler regions (Krivov et al. 2000). Larger grains would survive somewhat longer, but not more than a few tens of years due to the high collision rate in the inner disk. A large dust production rate ($\sim 10^{-8}$ $\mathcal{M}_{\oplus}$/yr) is thus needed to explain our observations, suggesting that major dynamical perturbations are currently ongoing in the Vega system. An attractive scenario would be an equivalent to the Late Heavy Bombardment that happened in the solar system in the 700 Myr following the formation of the planets (Hartmann et al. 2000), i.e., at a period compatible with the age of Vega (∼350 Myr). Such a bombardment, most probably triggered by the outward migration of giant planets (Gomes et al. 2005), could explain the presence of small grains around Vega both in its outer disk, due to an enhanced collision rate in this part of the disk, and in its inner disk, due to the high

number of comets sent toward the star by gravitational interaction with the migrating planets. Although the presence of giant planets around Vega has not been confirmed yet, Wyatt (2003) has suggested that the outward migration of a Neptune-sized body from 40 to 65 AU could explain the observed clumpy structure in Vega's outer disk.

5. Conclusion

In this paper, we have presented high precision visibility measurements obtained on Vega at the CHARA Array with the FLUOR beam-combiner. The presence of a significant deficit of visibility at short baselines with respect to a simple uniform disk stellar model led us to the conclusion that an additional source of K-band emission is present in the FLUOR field-of-view centred around Vega (1″ in radius), with an estimated excess of $1.29 \pm 0.19\%$ relative to the photospheric emission. Among the possible sources for this excess emission, the presence of dust grains in the close vicinity of Vega, heated by the star and radiating mostly in the near-infrared, is proposed as the most probable one. Vega, a prototypical debris-disk star surrounded by a large quantity of dust at about 85 AU, was already suspected by several authors to harbour warm dust grains arranged in an inner circumstellar disk. Previous studies were however limited to a precision of a few percent on the total infrared flux of the Vega system and therefore did not provide a precise estimation of the excess emission associated with the inner disk.

Thanks to our precise determination of the integrated K-band emission emanating from the inner 8 AU of the Vega debris disk, we were able to infer some physical properties of the dust, which is suspected to be mainly composed of sub-micronic highly refractive grains mainly concentrated in the first AU around Vega and heated up to 1700 K. An estimated dust mass of $8 \times 10^{-8}\ \mathcal{M}_\oplus$ and a fractional luminosity of $\sim 5 \times 10^{-4}$ are derived from our best-fit model. We propose that a major dynamical event, similar to the solar system Late Heavy Bombardment, might be the cause for the presence of small dust grains in the inner disk of Vega.

Acknowledgements. We thank P. J. Goldfinger and G. Romano for their assistance with the operation of CHARA and FLUOR respectively. The CHARA Array is operated by the Center for High Angular Resolution Astronomy with support from Georgia State University and the National Science Foundation, the W.M. Keck Foundation and the David and Lucile Packard Foundation. This research has made use of NASA's Astrophysics Data System and of the SIMBAD database, operated at CDS (Strasbourg, France).

References

Aufdenberg, J. A., Mérand, A., Coudé du Foresto, V., et al. 2006, ApJ, submitted
Augereau, J. C., Lagrange, A. M., Mouillet, D., Papaloizou, J. C. B., & Grorod, P. A. 1999, A&A, 348, 557
Aumann, H., Beichman, C., Gillett, F., et al. 1984, ApJ, 278, L23
Backman, D., & Paresce, F. 1993, in Protostar and Planet III, ed. E. Levy, & J. Lunine (Tucson: Univ. of Arizona Press), 1253
Baraffe, I., Chabrier, G., Allard, F., & Hauschildt, P. H. 1998, A&A, 337, 403
Bessel, M., & Brett, J. 1988, PASP, 100, 1134
Beust, H., & Morbidelli, A. 2000, Icarus, 143, 170
Blackwell, D. E., Leggett, S. K., Petford, A. D., Mountain, C. M., & Selby, M. J. 1983, MNRAS, 205, 897
Bohlin, R. C., & Gilliland, R. L. 2004, AJ, 127, 3508
Bordé, P., Coudé du Foresto, V., Chagnon, G., & Perrin, G. 2002, A&A, 393, 183
Campins, H., Rieke, G. H., & Lebofsky, M. J. 1985, AJ, 90, 896
Ciardi, D., van Belle, G., Akeson, R., Thompson, R., & Lada, E. 2001, ApJ, 559, 1147
Cohen, M., Walker, R. G., Barlow, M. J., & Deacon, J. R. 1992, AJ, 104, 1650
Coudé du Foresto, V., Bordé, P. J., Mérand, A., et al. 2003, in Interferometry in Optical Astronomy II, ed. W. Traub, Proc. SPIE, 4838, 280
Coudé du Foresto, V., Ridgway, S., & Mariotti, J.-M. 1997, A&AS, 121, 379
Cutri, R. M., Skrutskie, M. F., van Dyk, S., et al. 2003, VizieR Online Data Catalog, 2246, 0
Delfosse, X., Forveille, T., Ségransan, D., et al. 2000, A&A, 364, 217
Dent, W. R. F., Walker, H. J., Holland, W. S., & Greaves, J. S. 2000, MNRAS, 314, 702
di Folco, E., Thévenin, F., Kervella, P., et al. 2004, A&A, 426, 601
Dominik, C., & Decin, G. 2003, ApJ, 598, 626
Dommanget, J., & Nys, O. 2002, VizieR Online Data Catalog, 1269, 0
Dorschner, J., Begemann, B., Henning, T., Jaeger, C., & Mutschke, H. 1995, A&A, 300, 503
Fajardo-Acosta, S., Telesco, C., & Knacke, R. 1998, AJ, 115, 2101
Fajardo-Acosta, S. B., Stencel, R. E., Backman, D. E., & Thakur, N. 1999, ApJ, 520, 215
Gaidos, E., & Koresko, C. 2004, New Astron., 9, 33
Gomes, R., Levison, H. F., Tsiganis, K., & Morbidelli, A. 2005, Nature, 435, 466
Grün, E., Zook, H. A., Fechtig, H., & Giese, R. H. 1985, Icarus, 62, 244
Gulliver, A. F., Hill, G., & Adelman, S. J. 1994, ApJ, 429, L81
Guyon, O. 2002, A&A, 387, 366
Hanbury Brown, R., Davis, J., & Allen, L. 1974, MNRAS, 167, 121
Hanner, M. S. 1984, Adv. Space Res., 4, 189
Hartmann, W. K., Ryder, G., Dones, L., & Grinspoon, D. 2000, in Origin of the Earth and Moon, ed. R. M. Canup, & K. Righter (Tucson: Univ. of Arizona Press.), 493
Hauschildt, P. H., Allard, F., & Baron, E. 1999, ApJ, 512, 377
Hearnshaw, J. B. 1996, The Measurement of Starlight, Two Centuries of Astronomical Photometry (Cambridge: Cambridge University Press)
Heinrichsen, I., Walker, H. J., & Klaas, U. 1998, MNRAS, 293, L78
Hestroffer, D. 1997, A&A, 327, 199
Holland, W. S., Greaves, J. S., Zuckerman, B., et al. 1998, Nature, 392, 788
Kelsall, T., Weiland, J. L., Franz, B. A., et al. 1998, ApJ, 508, 44
Kervella, P., Ségransan, D., & Coudé du Foresto, V. 2004, A&A, 425, 1161
Kervella, P., Thévenin, F., Ségransan, D., et al. 2003, A&A, 404, 1087
Koerner, D. W., Sargent, A. I., & Ostroff, N. A. 2001, ApJ, 560, L181
Krivov, A. V., Mann, I., & Krivova, N. A. 2000, A&A, 362, 1127
Laor, A., & Draine, B. T. 1993, ApJ, 402, 441
Laureijs, R. J., Jourdain de Muizon, M., Leech, K., et al. 2002, A&A, 387, 285
Leggett, S. K., Bartholomew, M., Mountain, C. M., & Selby, M. J. 1986, MNRAS, 223, 443
Liu, W. M., Hinz, P. M., Hoffmann, W. F., et al. 2004, ApJ, 610, L125
Macintosh, B. A., Becklin, E. E., Kaisler, D., Konopacky, Q., & Zuckerman, B. 2003, ApJ, 594, 538
Mathis, J. S., Rumpl, W., & Nordsieck, K. H. 1977, ApJ, 217, 425
Mégessier, C. 1995, A&A, 296, 771
Mérand, A., Bordé, P., & Coudé du Foresto, V. 2005, A&A, 433, 1155
Metchev, S. A., Hillenbrand, L. A., & White, R. J. 2003, ApJ, 582, 1102
Mountain, C. M., Leggett, S. K., Selby, M. J., Blackwell, D. E., & Petford, A. D. 1985, A&A, 151, 399
Mozurkewich, D., Armstrong, J. T., Hindsley, R. B., et al. 2003, AJ, 126, 2502
Perrin, G. 2003, A&A, 400, 1173
Perryman, M. 2000, Rep. Prog. Phys., 63, 1209
Perryman, M. A. C. 1997, ESA SP Series, Vol. 1200, The HIPPARCOS and TYCHO catalogues. (Noordwijk, The Netherlands: ESA Publications Division)
Peterson, D. M., Hummel, C. A., Pauls, T. A., et al. 2004, in New Frontiers in Stellar Interferometry, ed. W. Traub, Proc. SPIE, 5491, 65
Reach, W. T., Morris, P., Boulanger, F., & Okumura, K. 2003, Icarus, 164, 384
Rieke, G. H., Lebofsky, M. J., & Low, F. J. 1985, AJ, 90, 900
Song, I., Caillaut, J.-P., Barrado y Navascuès, D., & Stauffer, J. 2001, ApJ, 546, 352
Su, K. Y. L., Rieke, G. H., Misselt, K. A., et al. 2005, ApJ, 628, 487
ten Brummelaar, T. A., McAlister, H. A., Ridgway, S. T., et al. 2005, ApJ, 628, 453
van Belle, G. T., Ciardi, D. R., Thompson, R. R., Akeson, R. L., & Lada, E. A. 2001, ApJ, 559, 1155
Weingartner, J. C., & Draine, B. T. 2001, ApJ, 548, 296
Wilner, D. J., Holman, M. J., Kuchner, M. J., & Ho, P. T. P. 2002, ApJ, 569, L115
Wyatt, M. C. 2003, ApJ, 598, 1321
Zubko, V. G., Mennella, V., Colangeli, L., & Bussoletti, E. 1996, MNRAS, 282, 1321